

**NATIONAL ADVISORY COMMITTEE
FOR AERONAUTICS**

REPORT No. 895

**ANALYSIS OF VARIATION OF PISTON
TEMPERATURE WITH PISTON DIMENSIONS AND
UNDERCROWN COOLING**

By J. C. SANDERS and W. B. SCHRAMM



1948

AERONAUTIC SYMBOLS

1. FUNDAMENTAL AND DERIVED UNITS

	Symbol	Metric		English	
		Unit	Abbrevia- tion	Unit	Abbrevia- tion
Length-----	<i>l</i>	meter-----	m	foot (or mile)-----	ft (or mi)
Time-----	<i>t</i>	second-----	s	second (or hour)-----	sec (or hr)
Force-----	<i>F</i>	weight of 1 kilogram-----	kg	weight of 1 pound-----	lb
Power-----	<i>P</i>	horsepower (metric)		horsepower-----	hp
Speed-----	<i>V</i>	{kilometers per hour-----	kph	miles per hour-----	mph
		{meters per second-----	mps	feet per second-----	fps

2. GENERAL SYMBOLS

<i>W</i>	Weight= mg	<i>v</i>	Kinematic viscosity
<i>g</i>	Standard acceleration of gravity= 9.80665 m/s^2 or 32.1740 ft/sec^2	ρ	Density (mass per unit volume)
<i>m</i>	Mass= $\frac{W}{g}$		Standard density of dry air, $0.12497 \text{ kg-m}^{-3}$ at 15° C and 760 mm ; or $0.002378 \text{ lb-ft}^{-3}$
<i>I</i>	Moment of inertia= mk^2 . (Indicate axis of radius of gyration k by proper subscript.)		Specific weight of "standard" air, 1.2255 kg/m^3 or 0.07651 lb/cu ft
μ	Coefficient of viscosity		

3. AERODYNAMIC SYMBOLS

<i>S</i>	Area	i_w	Angle of setting of wings (relative to thrust line)
S_w	Area of wing	i_t	Angle of stabilizer setting (relative to thrust line)
<i>G</i>	Gap	<i>Q</i>	Resultant moment
<i>b</i>	Span	Ω	Resultant angular velocity
<i>c</i>	Chord	<i>R</i>	Reynolds number, $\frac{Vl}{\mu}$ where l is a linear dimen- sion (e.g., for an airfoil of 1.0 ft chord, 100 mph, standard pressure at 15° C , the corresponding Reynolds number is 935,400; or for an airfoil of 1.0 m chord, 100 mps, the corresponding Reynolds number is 6,865,000)
<i>A</i>	Aspect ratio, $\frac{b^2}{S}$	α	Angle of attack
<i>V</i>	True air speed	ϵ	Angle of downwash
<i>q</i>	Dynamic pressure, $\frac{1}{2}\rho V^2$	α_o	Angle of attack, infinite aspect ratio
<i>L</i>	Lift, absolute coefficient $C_L = \frac{L}{qS}$	α_i	Angle of attack, induced
<i>D</i>	Drag, absolute coefficient $C_D = \frac{D}{qS}$	α_a	Angle of attack, absolute (measured from zero- lift position)
D_o	Profile drag, absolute coefficient $C_{D_o} = \frac{D_o}{qS}$	γ	Flight-path angle
D_i	Induced drag, absolute coefficient $C_{D_i} = \frac{D_i}{qS}$		
D_p	Parasite drag, absolute coefficient $C_{D_p} = \frac{D_p}{qS}$		
<i>C</i>	Cross-wind force, absolute coefficient $C_c = \frac{C}{qS}$		

REPORT No. 895

**ANALYSIS OF VARIATION OF PISTON
TEMPERATURE WITH PISTON DIMENSIONS AND
UNDERCROWN COOLING**

By J. C. SANDERS and W. B. SCHRAMM

**Flight Propulsion Research Laboratory
Cleveland, Ohio**

National Advisory Committee for Aeronautics

Headquarters, 1724 F Street NW, Washington 25, D. C.

Created by act of Congress approved March 3, 1915, for the supervision and direction of the scientific study of the problems of flight (U. S. Code, title 50, sec. 151). Its membership was increased to 17 by act approved May 25, 1948. (Public Law 549, 80th Congress). The members are appointed by the President, and serve as such without compensation.

JEROME C. HUNSAKER, Sc. D., Cambridge, Mass., *Chairman*

ALEXANDER WETMORE, Sc. D., Secretary, Smithsonian Institution, *Vice Chairman*

HON. JOHN R. ALISON, Assistant Secretary of Commerce.

DETLEV W. BRONK, Ph. D., President, Johns Hopkins University.

KARL T. COMPTON, Ph. D. Chairman, Research and Development Board, National Military Establishment.

EDWARD U. CONDON, Ph. D., Director, National Bureau of Standards.

JAMES H. DOOLITTLE, Sc. D., Vice President, Shell Union Oil Corp.

R. M. HAZEN, B. S., Director of Engineering, Allison Division, General Motors Corp.

WILLIAM LITTLEWOOD, M. E., Vice President, Engineering, American Airlines, Inc.

THEODORE C. LONNQUEST, Rear Admiral, United States Navy, Assistant Chief for Research and Development, Bureau of Aeronautics.

EDWARD M. POWERS, Major General, United States Air Force, Assistant Chief of Air Staff-4.

JOHN D. PRICE, Vice Admiral, United States Navy, Deputy Chief of Naval Operations (Air).

ARTHUR E. RAYMOND, M. S., Vice President, Engineering, Douglas Aircraft Co., Inc.

FRANCIS W. REICHELDERFER, Sc. D., Chief, United States Weather Bureau.

HON. DELOS W. RENTZEL, Administrator of Civil Aeronautics, Department of Commerce.

HOYT S. VANDENBERG, General, Chief of Staff, United States Air Force.

THEODORE P. WRIGHT, Sc. D., Vice President for Research, Cornell University.

HUGH L. DRYDEN, Ph. D., *Director of Aeronautical Research*

JOHN F. VICTORY, LL.M., *Executive Secretary*

JOHN W. CROWLEY, JR., B. S., *Associate Director of Aeronautical Research*

E. H. CHAMBERLIN, *Executive Officer*

HENRY J. E. REID, Eng. D., Director, Langley Aeronautical Laboratory, Langley Field, Va.

SMITH J. DEFRANCE, B. S., Director, Ames Aeronautical Laboratory, Moffett Field, Calif.

EDWARD R. SHARP, Sc. D., Director, Lewis Flight Propulsion Laboratory, Cleveland Airport, Cleveland, Ohio

TECHNICAL COMMITTEES

AERODYNAMICS
POWER PLANTS FOR AIRCRAFT
AIRCRAFT CONSTRUCTION

OPERATING PROBLEMS
INDUSTRY CONSULTING

Coordination of Research Needs of Military and Civil Aviation

Preparation of Research Programs

Allocation of Problems

Prevention of Duplication

Consideration of Inventions

LANGLEY AERONAUTICAL LABORATORY,
Langley Field, Va.

LEWIS FLIGHT PROPULSION LABORATORY,
Cleveland Airport, Cleveland, Ohio

AMES AERONAUTICAL LABORATORY,
Moffett Field, Calif.

Conduct, under unified control, for all agencies, of scientific research on the fundamental problems of flight

OFFICE OF AERONAUTICAL INTELLIGENCE,
Washington, D. C.

Collection, classification, compilation, and dissemination of scientific and technical information on aeronautics

REPORT No. 895

ANALYSIS OF VARIATION OF PISTON TEMPERATURE WITH PISTON DIMENSIONS AND UNDERCROWN COOLING

By J. C. SANDERS and W. B. SCHRAMM

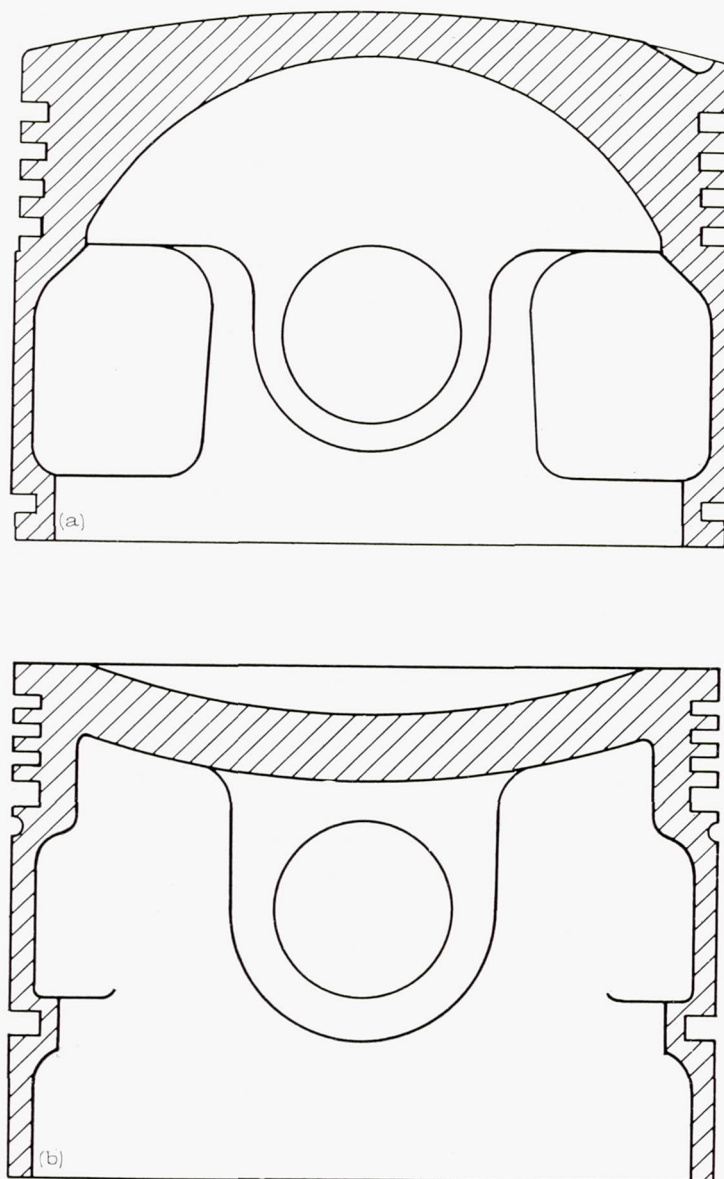
SUMMARY

A theoretical analysis is presented that permits estimation of the changes in piston-temperature distribution induced by variations in the crown thickness, the ring-groove-pad thickness, and the undercrown surface heat-transfer coefficient. The analysis consists of the calculation of operating temperatures at various points in the piston body on the basis of the experimentally determined surface heat-transfer coefficients and boundary-region temperatures, as well as arbitrarily selected surface coefficients. Surface heat-transfer coefficients were estimated from the internal temperature gradients obtained by hardness surveys of aluminum pistons that had been operated under severe conditions in a liquid-cooled, single-cylinder, $5\frac{1}{2}$ - by 6-inch test engine.

The results of the analysis indicate that many piston-cooling problems can be satisfactorily investigated by analytical methods when boundary conditions are known. Control of piston-temperature distribution by design alteration is limited where undercrown cooling is insufficient; but under conditions of adequate undercrown cooling, temperature distribution can be controlled. The heat balance for the piston-cooling load may indicate preponderance of flow in the direction of the cylinder wall or the crankcase atmosphere, but in either case, it is not a criterion of satisfactory temperature distribution.

INTRODUCTION

Previous investigations of piston-temperature control and heat-transfer characteristics (references 1 to 7) have led to divergent concepts of the piston-cooling process from which two generally distinct design principles have evolved. A typical piston design, which is based on the theory that heat dissipation occurs primarily through the piston rings, the ring lands, and the skirt to the cylinder wall, is illustrated in figure 1 (a). This general design, developed from extensive experimental and theoretical research, necessarily embodies a highly conductive heat-flow path from the crown to the ring-groove and skirt sections. This design was successful in maintaining reasonable crown and ring-belt temperatures at the relatively low specific power outputs encountered at the time of its development. (See references 1 and 2.) The heat balances reported in references 1 and 2 indicate that the amount of undercrown cooling was very small. Theoretical analyses (references 3 and 4), which



(a) Cooling to cylinder wall.

(b) Cooling to crankcase atmosphere.

FIGURE 1.—Piston design suitable for cooling to cylinder wall and to crankcase atmosphere.

assumed negligible undercrown heat transfer, confirmed the results observed in the experimental work.

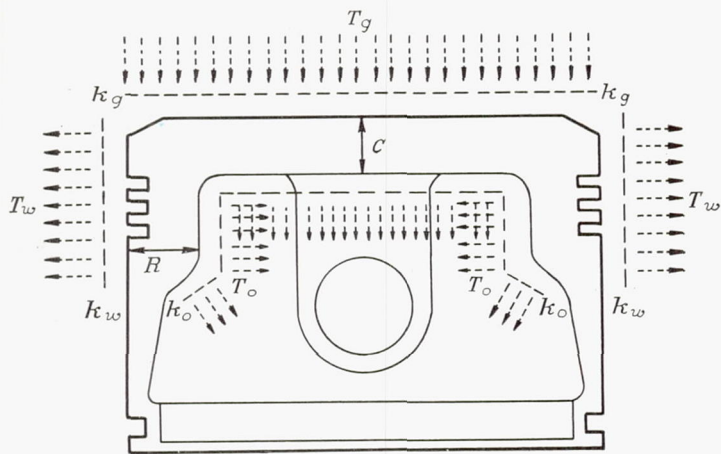


FIGURE 2.—Variables and heat-flow paths considered in analysis.

Another distinct type of piston design that has been developed for many engines of relatively high specific output is illustrated in figure 1 (b). Successful application of this design depends, for most purposes, upon the inherent capacity of some types of engine for natural undercrown convection cooling, or in other types upon the auxiliary cooling supplied by special oil jets directed at the undercrown surface. Representative investigations of this design are described in references 5 to 7.

Theoretical analysis, based on experimentally determined surface heat-transfer coefficients, seemed likely to disclose generally applicable trends that would aid qualitative solution of piston-cooling problems.

Calculations were therefore made at the NACA Cleveland laboratory in 1945 to estimate the effect of crown and ring-groove-pad thickness on piston-temperature distribution for several values of the undercrown-surface heat-transfer coefficient. The surface coefficients for the calculations were estimated from hardness surveys (references 7 and 8) of pistons that had been operated in a single-cylinder, liquid-cooled, 5½- by 6-inch test engine. Calculations were also made with arbitrarily selected surface coefficients to permit extension of the range of the analysis.

PISTON-COOLING PROCESS

The piston body is connected to the working fluid, the cylinder wall, the undercrown atmosphere, and the connecting rod through conductive films, and to the other combustion chamber surfaces, valves, and parts of the crankcase and crankshaft assembly by radiation. The temperatures of these regions may be initially considered independent variables so far as the piston-temperature analysis is concerned. The piston becomes a connecting link between the heat sources and the heat sinks, and temperature distribution becomes a dependent element.

The variables shown in figure 2 were selected for the analysis. The boundary-temperature conditions are the wall temperature, the temperature of the undercrown air and oil mixture, and the effective gas temperature for the combustion-chamber surface of the piston, which are denoted T_w , T_o , and T_g , respectively. The piston body is connected to these regions through conductive films represented by the surface coefficients k_w , k_o , and k_g . In order to make the solution representative of an actual operating condition,

these temperatures and coefficients were estimated from experimental data. The most significant design changes can be represented by variations in crown thickness C and ring-groove-pad thickness R , inasmuch as it is relatively simple to vary the thermal conductivity of various paths through the piston by selecting different combinations of these dimensions. The calculations yield temperatures for a number of points throughout the piston, but the presentation of results includes only values for the significant center-crown and ring-groove-pad temperatures.

THEORETICAL ANALYSIS

Description of network.—The analysis is limited to a two-dimensional system that may be revolved to form a complete cylindrical body of revolution. As a result of this limitation, the hot spot on the crown surface is shifted to the geometric center and the calculated temperature distribution of the body is concentric with the geometric center. The two-dimensional analysis precludes consideration of the conductive path through the pin bosses to the connecting rod and to parts of the upper-skirt section. The additional simplifications are the assumption of a perpendicular junction of the crown and the ring-groove-pad sections and elimination of the lower piston-skirt section.

The body of revolution is subdivided into simple geometric sections that are replaced by a two-dimensional network of paths connecting various points for which the temperatures are calculated. The relation of the network to the piston body is shown in figures 3 and 4 (a). Figure 3 illustrates the network as it would appear in a transparent sector of the assumed body of revolution. Points A and 3 represent the center-crown and ring-groove-pad temperatures, respectively, and the computed data for these points are used in the final presentation.

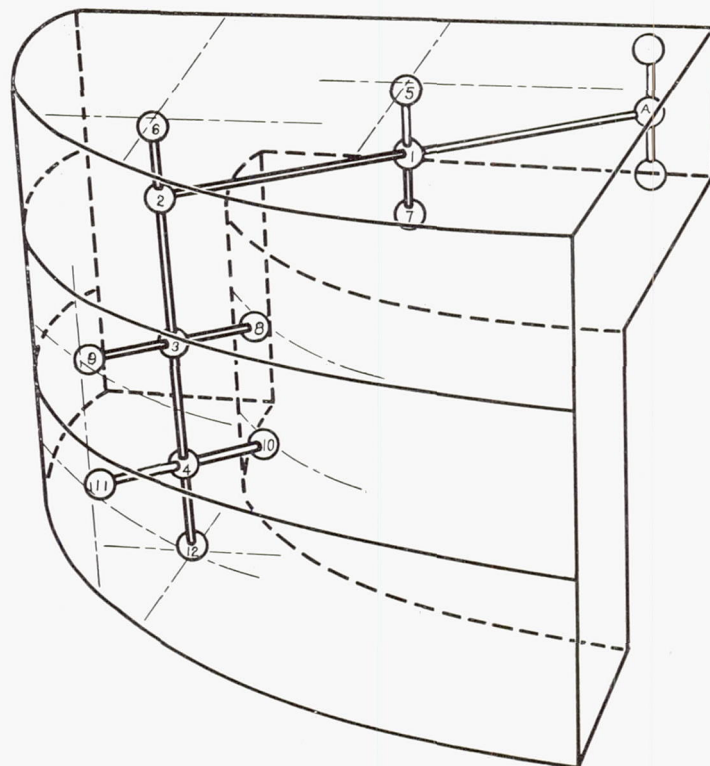


FIGURE 3.—Thermal network enclosed in sector of assumed body of revolution.

Heat is added and removed through the point on each surface at which the heat flow may be assumed concentrated, and the temperature of the point is assumed to be the equivalent mean temperature of the surface being considered. The internal points and paths of the network form heat-flow paths between the boundaries, as shown by the arrows in figure 4 (a), and it is through study of the changes affected in the resistance of these paths by design changes that the effect on temperature distribution is estimated. The heat dissipated from the lower piston-skirt section is generally quite small because of the limited temperature gradient that exists between it and the cylinder wall even with low values of undercrown heat transfer; it was therefore considered reasonable to approximate the heat-flow path from the upper body of the piston to the lower-skirt section by applying the undercrown coefficient in the region of point 12 (fig. 4 (a)) to the annular area, represented by the cross section at the junction of the body and the skirt. The thermal conductivities of the rings, the ring lands, and the surface films in the immediate area of the ring belt are combined and applied in the analysis as an over-all coefficient because the hardness surveys used to estimate the surface coefficients were inadequate for a close study of the ring grooves and the ring lands. No path connects point 2 with the cylinder-wall surface because temperature distributions obtained by hardness surveys indicate that, as a result of the relatively large relief machined on the outside diameter of the top land of the piston used in this investigation, there is no wall contact and little or no radial temperature gradient in this area during normal operation. Under some conditions, it may be necessary to include this path in the network.

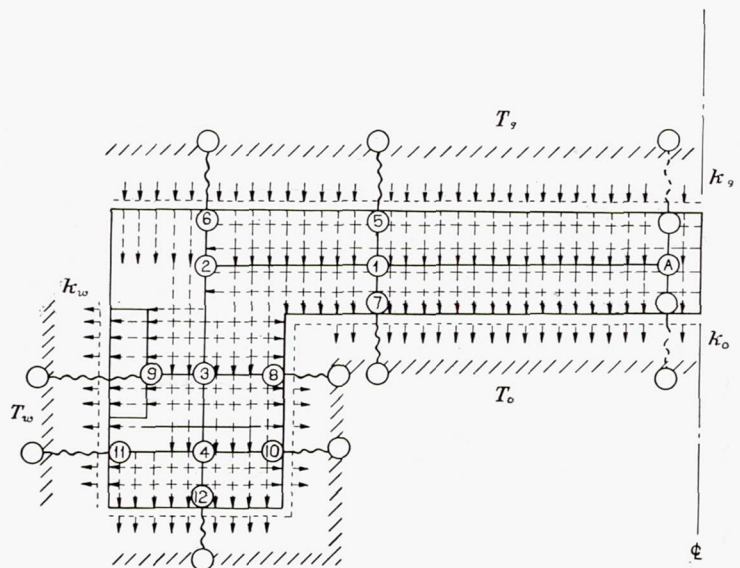
A solution for temperature distribution may be obtained by simultaneous equations presented in this analysis, by relaxation methods, or by substitution of data in an electric network analyzer (reference 9).

Network theory.—It is first necessary to develop equations that relate the temperatures of adjacent points or boundaries in terms of the over-all thermal conductivities of the connecting network paths. By combination of the individual thermal conductivities of the contributing network paths, the 12-point network can be reduced to a simplified 4-point network, which is illustrated in figure 4 (b). The network paths that connect the central points to the boundary-region points now include conductivity of the piston body and the surface film. The conductivity of each path is made equal to that of the piston section or surface film that it replaces and is related to temperature differential and heat flow by the steady-state equation

$$q = \frac{kA}{x} \Delta T \quad (1)$$

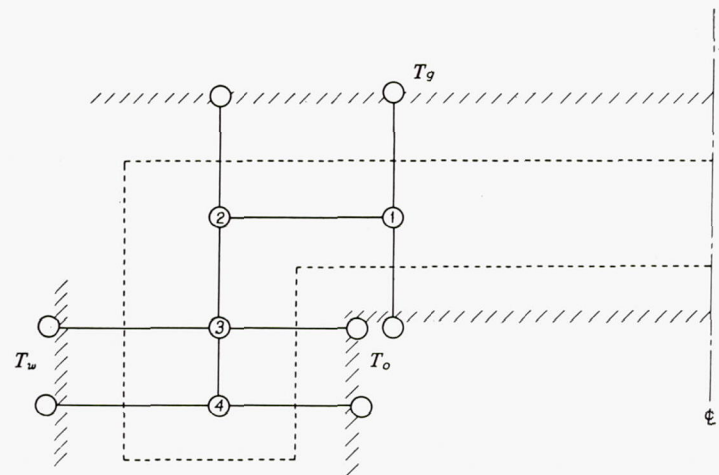
where

- q heat-transfer rate between points, (Btu/(hr))
- k thermal-conductivity coefficient of metal, (Btu/(hr) (sq in.) (°F/in.))
- A mean cross-sectional area, (sq in.)
- x mean thickness of section, (in.)
- ΔT temperature gradient between points, (°F)



(a)

(a) View showing 12-point network and heat-flow paths.



(b)

(b) View showing network after reduction to 4 basic points.

FIGURE 4.—Cross section of assumed body of revolution.

When a surface film is considered, the term k/x is replaced by k' , which is the surface heat-transfer coefficient for the film in (Btu/(hr)(sq in.)(°F)).

The following equations, which are based on equation (1), may be established for point 1 in the reduced network shown in figure 4 (b):

$$q_{g-1} = K_{g-1}(T_g - T_1) \quad (2)$$

$$q_{1-2} = K_{1-2}(T_1 - T_2) \quad (3)$$

$$q_{1-o} = K_{1-o}(T_1 - T_o) \quad (4)$$

When a boundary is referred to, the subscripts g , o , and w denote the gas, the undercrown regions, and the cylinder wall, respectively.

In these and in subsequent equations, K is the over-all conductivity in (Btu/(hr)(°F)) between the points and the boundary regions denoted by the subscripts and will be derived from the geometry of the section and the values for k and k' .

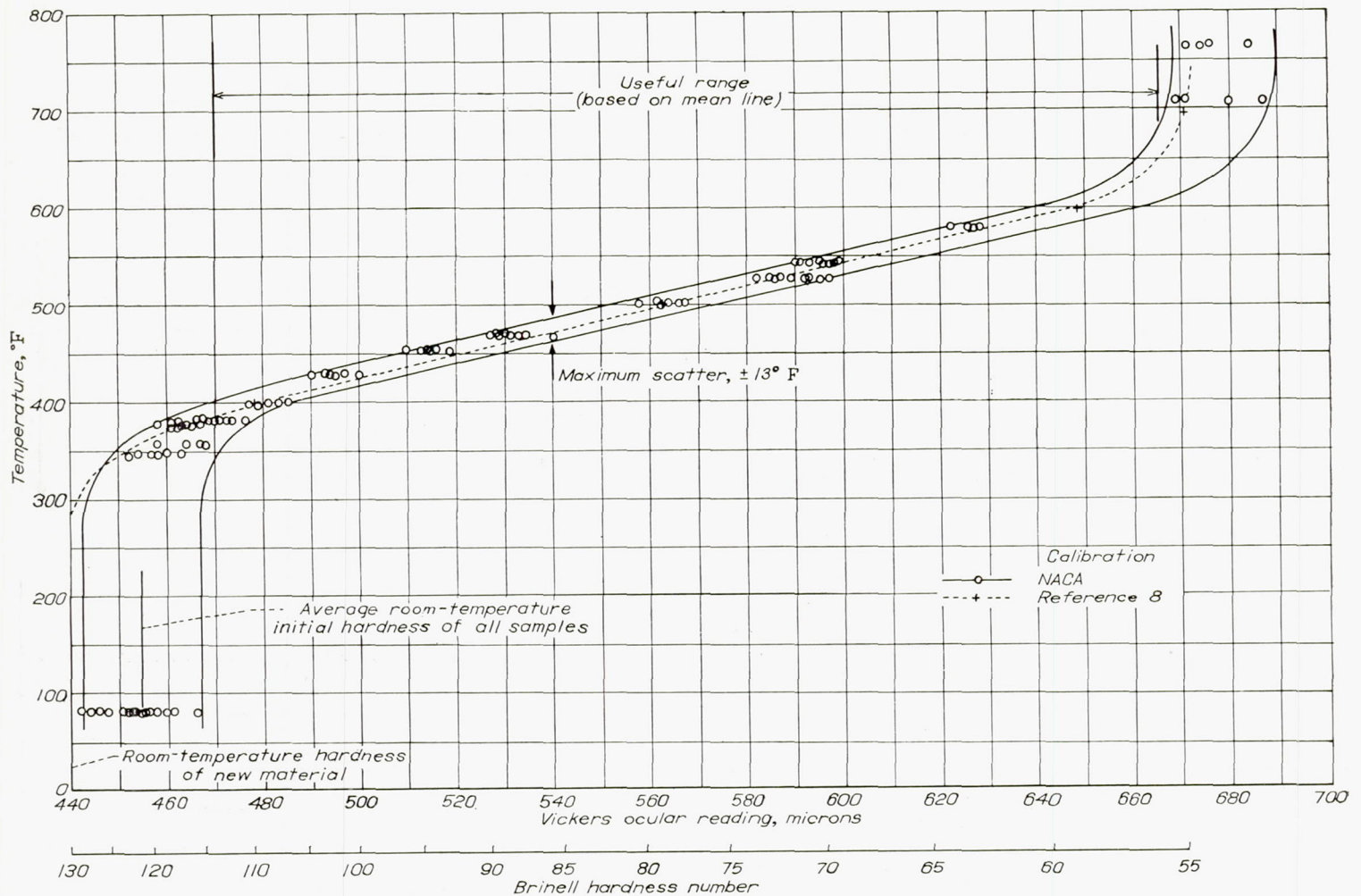


FIGURE 5.—NACA hardness calibration of 32S-T aluminum alloy for 5-hour period of overaging. Ball diameter, 2 millimeters; two-thirds objective; load, 20 kilograms.

Because the summation of the heat flow into and away from a point is zero,

$$K_{g-1}(T_g - T_1) - K_{1-2}(T_1 - T_2) - K_{1-o}(T_1 - T_o) = 0 \quad (5)$$

When this equation is solved for T_1 , the following expression is obtained:

$$T_1 = \frac{K_{g-1}T_g + K_{1-2}T_2 + K_{1-o}T_o}{K_{g-1} + K_{1-2} + K_{1-o}} \quad (6)$$

By a similar process, the equations for the three other basic points in figure 4 (b) may be established. The four equations were solved simultaneously for one of the piston temperatures in terms of the boundary-region temperatures and the conductivities of all the network paths; the solution was then reversed to evaluate the remaining temperatures. Inasmuch as point 1 is located where the heat flows may be assumed concentrated, T_1 represents the mean temperature of the center-crown section. The local value T_A , which represents the center crown or hot-spot temperature (point A, fig. 3), can then be computed from the local crown and undercrown-surface coefficients and T_1 .

DETERMINATION OF BOUNDARY CONDITIONS

Two pistons were operated in a single-cylinder, liquid-

cooled $5\frac{1}{2}$ - by 6-inch test engine for 5 hours at the following conditions:

Speed, rpm	3000
Indicated mean effective pressure, lb/sq in.	310
Fuel-air ratio	0.10
Combustion-air temperature, °F	250
Coolant-in temperature, °F	250
Undercrown oil flow from directed jets, lb/min	2.2-2.5
Undercrown oil-jet temperature, °F	220

The undercrown oil flow from directed jets was set at 2.2 to 2.5 pounds per minute in accordance with estimates of the undercrown oil flow normally encountered in a multicylinder engine. Comparison of hardness surveys made for pistons from multicylinder and single-cylinder engines indicates that except for the area of jet impingement, the specified flow from the jets closely reproduces in the piston of a single-cylinder engine the temperature distribution obtained in those of a multicylinder engine for the same engine operating conditions.

BOUNDARY TEMPERATURES

The values for T_w and T_o selected from the operating data were 260° and 220° F, respectively. In the absence of specific data for the effective gas temperature for the piston crown, a value of 1200° F was selected for T_g on the basis of data for a cylinder head reported in reference 10.

BOUNDARY-SURFACE COEFFICIENTS

An indirect technique for determination of local surface coefficients from internal-temperature gradients, which are determined from age-hardening characteristics, has been available for some time but is not widely used. The aluminum-copper alloys commonly used for piston forgings possess age-hardening characteristics that are sufficiently reproducible for a limited range to permit calibration on the basis of time, temperature, and hardness. Data for this calibration must first be obtained by heating samples under accurate control conditions. If a piston is installed in the engine at its condition of maximum hardness and run at constant engine conditions for a specified length of time, the internal temperature gradients can be determined by cutting the piston along the desired planes, making a hardness survey, and applying the calibration. During operation in the engine, each point

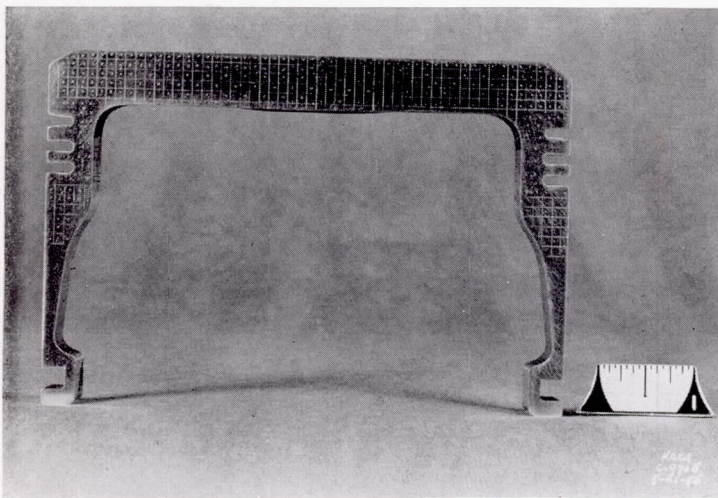


FIGURE 6.—Piston section after hardness survey.

in the piston is aged at approximately constant temperature for the specified time, thereby reproducing the operation performed on the sample in the furnace. This method was used by Gossiau (reference 7) for isothermal mapping of piston sections and for qualitative study of piston-heat flow and design modifications.

The calibration for 32S-T aluminum alloy in figure 5 gives the relation between operating temperature and measured room-temperature hardness for 5 hours at the specified temperatures. The scale of Brinell hardness number corresponding to the Vickers ocular readings for the specified load, the indenter, and the microscope objective is also given. The indicated scatter band of $\pm 13^\circ\text{F}$ represents unfavorable conditions because the samples cut from a used piston were individually solution-treated and aged, thus introducing variations in heat treatment in addition to the scatter normally encountered from physical variations in the metal structure of a single large sample. This variation is evidenced by the wide scatter of room-temperature initial hardness, which would ordinarily be very close to a Brinell hardness number of 130. Comparison with data from reference 8 indicates that within most of the useful range, the mean hardness-temperature relation is not critically sensitive to the past

history of the sample. In hardness surveys made after operation of a new piston, most of the data fell within a scatter band of $\pm 5^\circ\text{F}$, although occasional points were $\pm 50^\circ\text{F}$ from the mean of adjacent readings.

In order to obtain the surface heat-transfer coefficient, the following procedure was used: The piston was cut along a plane normal to the piston surface to be analyzed and a hardness survey was made (fig. 6). A plot of these data for two parallel rows 0.05 and 0.15 inch from the crown surface, after conversion from hardness values to temperature values, is shown in figure 7 (a); a similar plot is shown in figure 7 (b) for two rows 0.10 and 0.20 inch from the undercrown surface. In order to minimize the effects of scatter, smooth curves representing temperature variation are drawn through the points in each row. The vertical distance between the two curves represents in each case the temperature gradient at each station across the 0.10-inch-thick layer of metal and may be substituted in the Fourier equation with the thermal conductivity of the metal (8 Btu/(hr) (sq in.) ($^\circ\text{F}/\text{in.}$)) to solve for the heat flow at each station perpendicular to the piston surface being analyzed. It is assumed that this normal component does not change in traversing the remaining distance to the surface. The numerical heat-flow value obtained by this operation is again substituted in the Fourier equation with the temperature gradient from the surface to the boundary region to calculate the surface heat-transfer coefficient at each station.

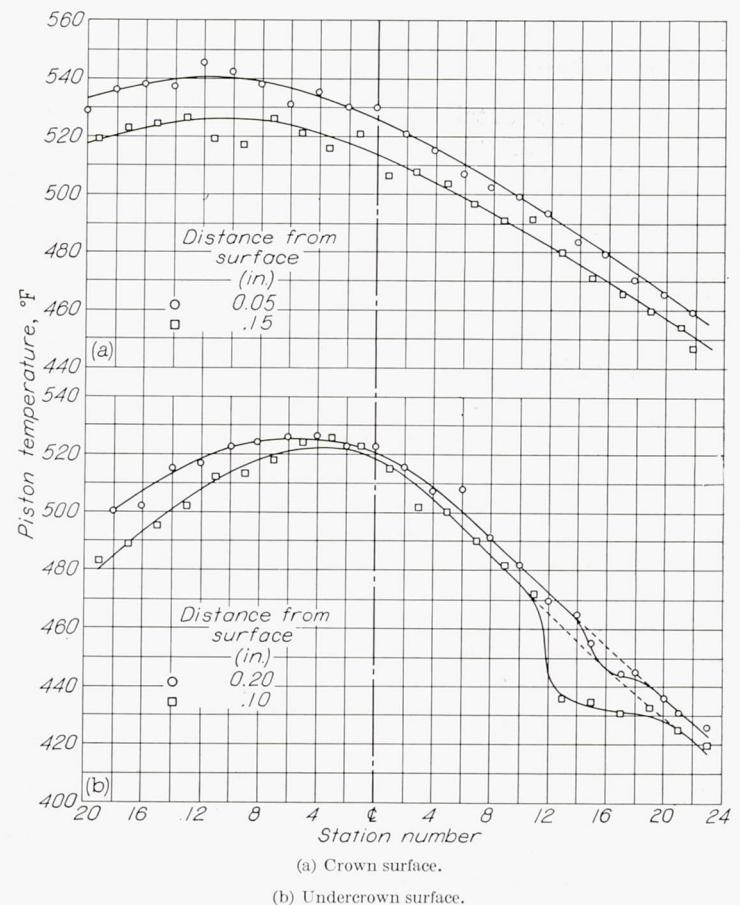


FIGURE 7.—Piston temperatures obtained by hardness measurements along two rows parallel to undercrown and crown surfaces of piston.

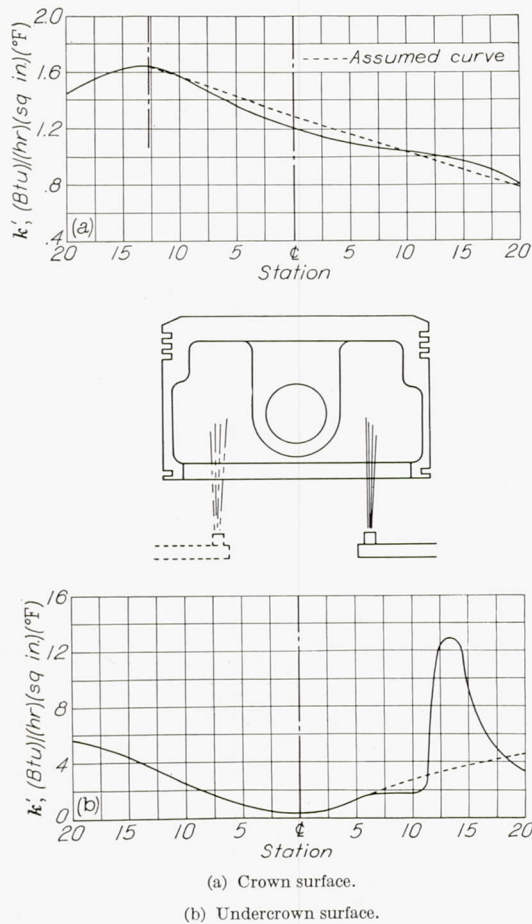


FIGURE 8.—Local heat-transfer coefficient for undercrown and crown surfaces of piston.

The coefficients obtained from the data shown in figure 7 appear in figure 8. The undercrown surface of the piston was cooled by high-velocity oil jets, one of which struck the piston at a point in the plane along which the section was cut. The high local coefficient at this point was not directly considered in selecting a representative value for the calculations. The dashed lines in figures 7 (b) and 8 (b) show the results of neglecting this local value; the final selection was slightly higher than the average obtained on the basis of this approximation.

In figure 8 (a), the coefficients for the crown surface derived from the data in figure 7 (a) indicate that the hot spot falls opposite the region of maximum surface coefficient. The center line was transferred to the peak of the curve and representative values for the calculations were selected from the assumed curve at the appropriate radii, as shown in figure 8 (a).

The experimentally determined average coefficients used in the calculations are listed in table I. These values are representative of a number of pistons that were analyzed with the exception of the coefficient for the section behind the ring grooves, which was estimated from the difference between the known heat input at the crown surface and the known dissipation from the undercrown, ring-belt, and skirt surfaces. Because the surface coefficients were determined

from the normal temperature gradients, they may include a radiation factor of undetermined magnitude, which is rightly included in the analysis of temperature distribution.

TABLE I—EXPERIMENTALLY DETERMINED AVERAGE COEFFICIENTS

Location	k' , (Btu)/(hr)(sq in.)(°F)
Combustion gas to center-crown section.....	1.2
Combustion gas to peripheral-crown section.....	.9
Undercrown section to crankcase atmosphere.....	3.0
Section behind ring-groove pad to crankcase atmosphere.....	1.3
Conductivity through rings and grooves including films to cylinder wall.....	1.3
Upper-skirt section to cylinder wall.....	2.5

A degree of experimental confirmation is found in the data of reference 11 on surface coefficients between a heated piston and a reciprocating sleeve. A coefficient of approximately 3.2 (Btu/hr) (sq in.) (°F) was computed from correlation data in reference 11 as compared with a value of 2.5 (Btu/hr) (sq in.) (°F) reported herein.

PROCEDURE AND ACCURACY

In order to check the network equations and the suitability of the coefficients, a series of preliminary calculations were made to check the temperature distribution and the heat balance of a piston that was used for the hardness survey. Any large error in a coefficient would appear as distortion of the temperature distribution, and after small adjustments the coefficients given in table I were selected as satisfactory.

The temperatures obtained in the calculation are compared with the temperature distribution obtained by a hardness survey in figure 9. The values of observed temperature in the section perpendicular to the pin axis are used for comparison with calculated values because they are influenced the least by the pin bosses. The shift of the peak-

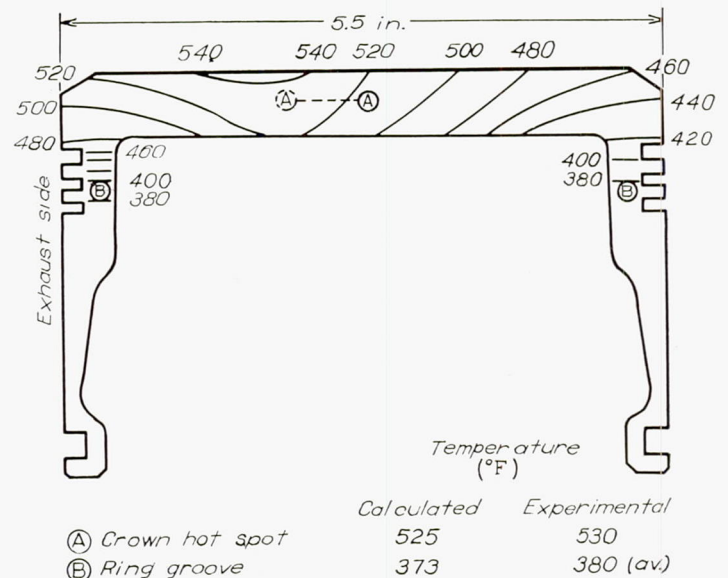


FIGURE 9.—Temperature distribution obtained by hardness measurements and comparison of measured and calculated values. (All values in °F unless otherwise indicated.)

temperature location toward the exhaust side of the piston makes direct comparison impossible inasmuch as the isothermals in the calculated example are concentric with the geometric center. The computed value of T_A (525°F) based on local surface coefficients at the center, however, represents the hot-spot temperature at the location between the crown and the undercrown surfaces indicated by the symbol A. The final plots were made using data for T_A based on average coefficients. Local coefficients were not used at the center of the crown for the calculations made with assumed average undercrown coefficients because the variation of local undercrown coefficients is unknown for the other operating conditions assumed. The data for center-crown temperature in figures 10 to 12 are lower than the hot-spot temperature by about 10° to 15°F as a maximum. The calculated temperature distribution obtained with the experimental boundary temperatures and coefficients and with measured piston dimensions was selected as the reference point for comparison of distributions obtained with altered boundary conditions and altered internal dimensions.

A series of calculations were made to investigate the changes induced in the temperature distribution by variations in crown and ring-groove-pad thicknesses. The surface coefficients and boundary temperatures were kept constant at the experimentally established values. The range of the analysis was then extended by arbitrary variation of the average undercrown surface coefficients to determine the effect of change in the undercrown-cooling condition for the same range of design dimensions. The trends calculated by arbitrary variation of the boundary coefficient may be considered only as a qualitative evaluation. It was assumed that the other coefficients remain constant; during actual operation, however, the large changes in piston temperature that result from variation in the undercrown coefficient would probably affect other boundary and surface conditions.

RESULTS AND DISCUSSION

The analysis was made for a particular range of boundary conditions that represent severe operating conditions; the results may therefore not be numerically representative of more moderate operating conditions. The trends shown are believed, however, to be generally representative and applicable to most installations if at least a qualitative evaluation of the particular boundary conditions that may be encountered is assumed. Unique conditions found in some types of engine may require entirely different concepts of the cooling process and appropriate design requirements. In any case, if the boundary conditions can be estimated, a process similar to this analysis may be of assistance in indicating possible methods for improving performance of the piston.

The results of the calculations are presented in the form of isometric projections to show the relation of the crown thickness, the ring-groove-pad thickness, and the undercrown-surface coefficient to operating temperature.

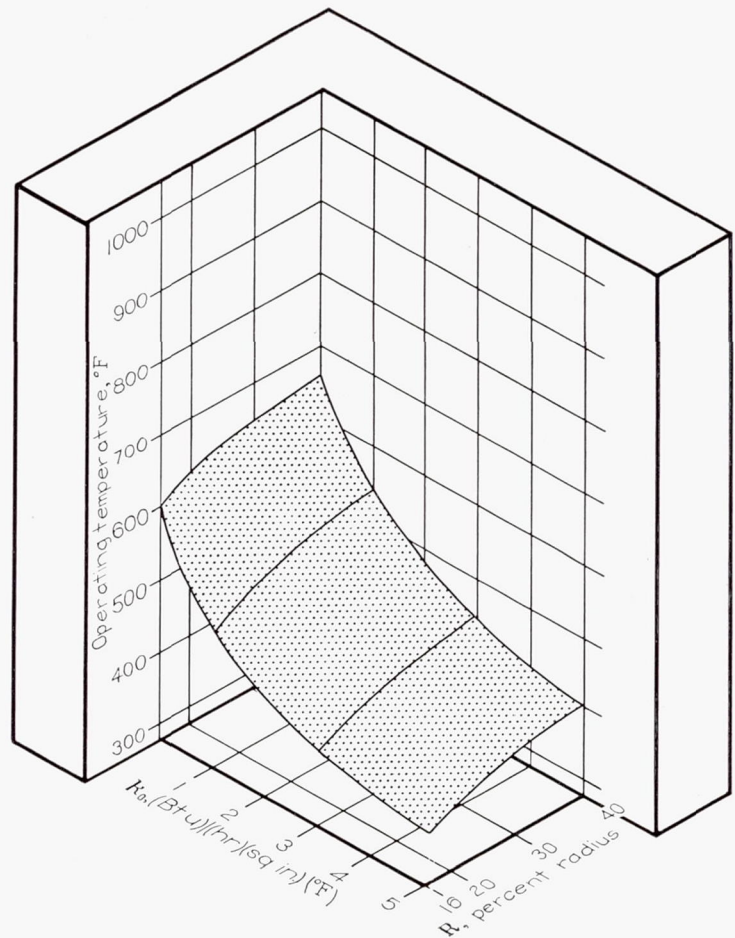


FIGURE 10.—Variation of calculated ring-groove-pad temperature with undercrown-surface coefficient k_o and ring-groove-pad thickness R . Crown thickness C , 30 percent of piston radius r .

The crown thickness C and ring-groove-pad thickness R are expressed as percentages of the radius of the cylinder bore to facilitate comparison between pistons of various design.

The surface shown in figure 10 represents the variation of ring-groove-pad temperature with the undercrown-surface coefficient k_o and ring-groove-pad thickness R at a constant value of crown thickness C of 30 percent of the radius r . All boundary conditions, with the exception of k_o , are also constant and represent the previously given operating conditions and the data in table I. From any point on the shaded surface that represents operating temperature, an increase in k_o or a decrease in R results in a decrease in ring-groove-pad temperature. The rate of change of temperature with k_o is greatest at low values of k_o , which indicates that the greatest improvements are obtained with the first increments. It is also apparent that sensitivity of ring-groove-pad temperature to R is greatest in the range of thin sections.

The light shaded surface in figure 11 represents the center-crown temperature for the same conditions and for the same range of variables. The effect of k_o on crown temperature is more pronounced than on ring-groove-pad temperature at the lower values, but the crown-temperature reduction obtained with successive increments in k_o rapidly diminishes.

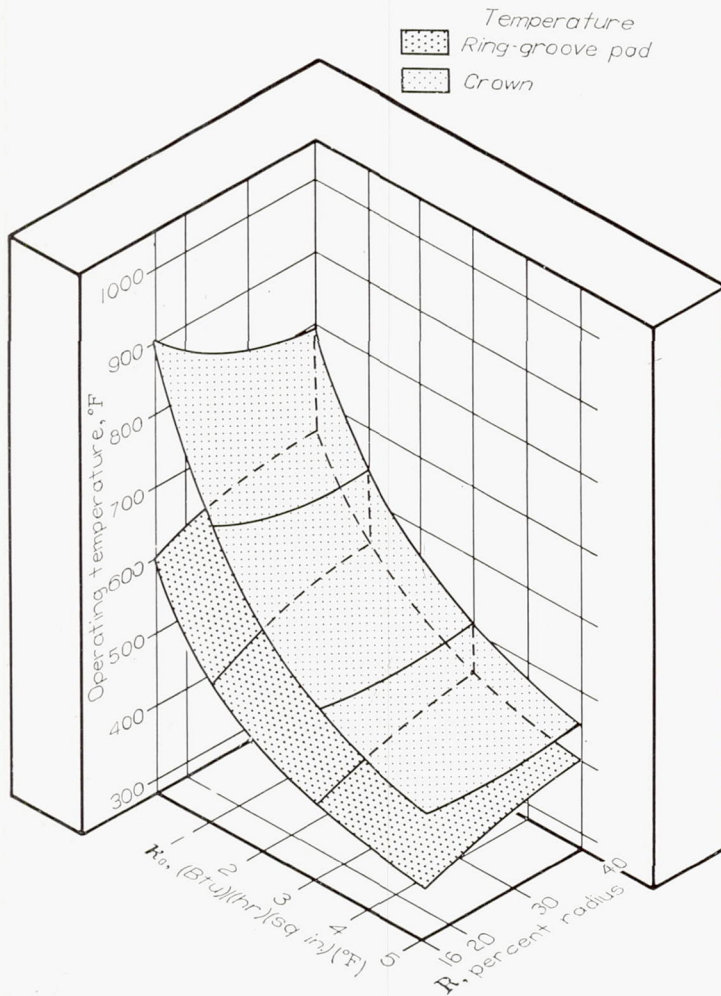


FIGURE 11.—Variation of calculated crown and ring-groove-pad temperatures with under-crown-surface coefficient k_o and ring-groove-pad thickness R . Crown thickness C , 30 percent of piston radius r .

The variation of crown temperature with R is negligible in the range above the experimentally determined value for k_o of 3 (Btu/(hr)(sq in.)(°F)), but becomes more pronounced for the lower values of k_o , particularly with very thin ring-groove-pad sections.

In order to present a more complete picture of this process, the data computed for a thin crown section of 8 percent of the radius r may be superimposed on figure 11 resulting in the final plot shown in figure 12. In this figure, the temperatures obtained for a thick crown (30-percent r) are represented by the light shaded surfaces and for a thin crown (8-percent r) by the dark shaded surfaces. Variations of k_o and R with the thin crown have the same effect on ring-groove-pad temperature as with the thick crown, although the temperature level is lower throughout the range. A decrease in crown thickness C to 8 percent results in a large increase in crown temperature at very low values of k_o (0 to 1 Btu/(hr)(sq in.)(°F)), and a decrease in crown temperature with high values of k_o (3 to 5 Btu/(hr)(sq in.)(°F)). It is clear from figure 12 that the undercrown coolant has a dual role in piston-temperature control. In addition to the direct-cooling effect, the effect of a change in crown thickness is so modified by a change in k_o that the trend of crown-temperature variation is reversed. For any particular value of R , there is a value of k_o at which crown thickness has no influence

over crown temperature. This transition point marks, in a sense, the change from primary cooling through the cylinder wall to primary cooling through the undercrown atmosphere; it is apparent that the design criterions are different in each case.

The early experimental work by Gibson (reference 1) and Baker (reference 2), from which evolved the common design of a light-alloy piston characterized by heavy sections and a generous undercrown radius, was done in engines of relatively low specific output. The heat balances reported indicate that the investigation was performed under conditions that produced a low undercrown-surface coefficient; because crown-temperature control was the primary objective, the design selected made the best possible use of the available cylinder-wall cooling. The reason is clearly shown in figure 12; for low values of k_o , the lowest crown temperatures are obtained with thick crown and ring-groove-pad sections because the maximum conductivity of the path from heat source to coolant is obtained. It is also apparent in figure 12 that this high conductivity results in maximum

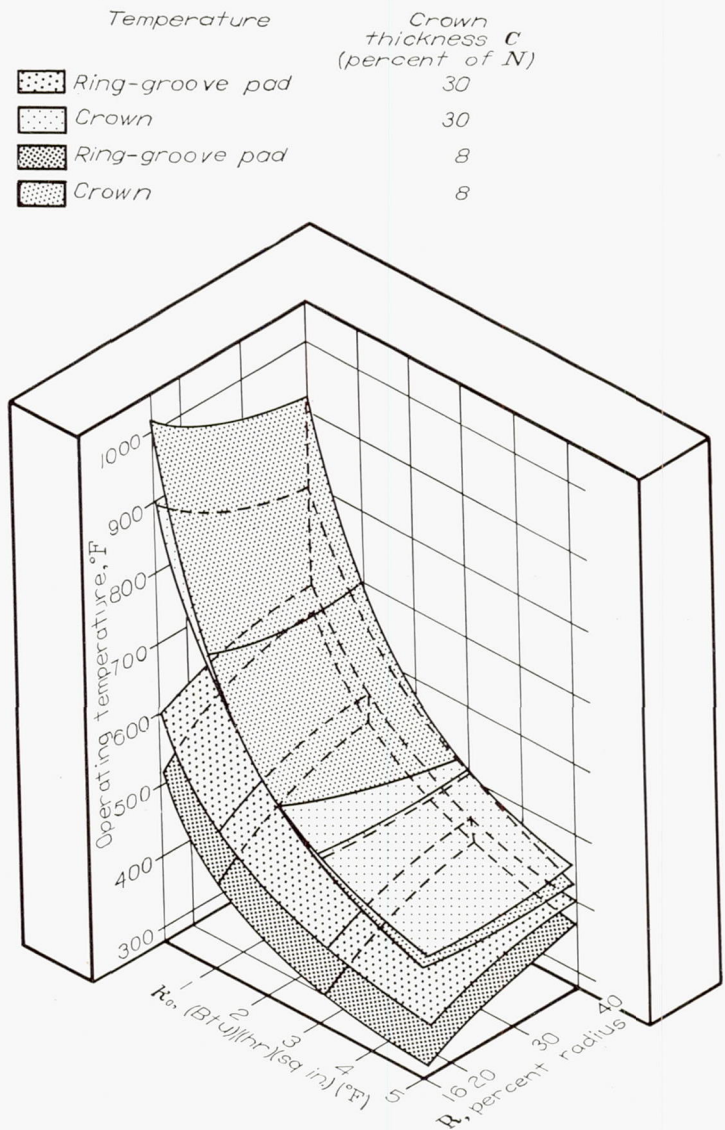


FIGURE 12.—Variation of calculated crown and ring-groove-pad temperatures with under-crown-surface coefficient k_o and ring-groove-pad thickness R .

ring-groove-pad temperatures. Conversely, if ring-groove-pad temperature is reduced by decreasing the conductivity of this path, excessive crown temperature is likely to result. The temperatures indicated in figure 12 for the condition of $k_o=0$ are very sensitive to the value assumed for T_g in the calculations and therefore unreliable except to show the trends and the relative values.

In many cases, the increase in engine performance resulting from normal development was limited by ring distress caused in part by excessive ring-groove-pad temperatures encountered when the conventional design was retained. This distress did not necessarily appear in all types of engine. Although some designers were forced to search for an improved method of temperature control, others were able to continue the use of the conventional design. It is believed that this digression was largely due to increases in rotative speed and the wider use of high-pressure oil systems that combined their individual effects to increase the natural undercrown cooling.

The results of the calculations show that effective control of piston temperature can be achieved through increase in the undercrown coefficient and that the greatest gains are obtained with the first increments. This observation is confirmed in references 5 and 6 as well as by unreported experiments made at this laboratory. It can be seen in figure 2 that the addition of adequate undercrown cooling so alters the operating conditions that the relatively long radial heat-flow path from the center of the crown to the ring-groove pad becomes of negligible importance. The heat-flow path to the primary coolant under the crown is made short and could not very well result in severe axial temperature gradients. In addition, the auxiliary coolant may impinge indirectly on the area behind the ring-groove pad and provide a second path for cooling from this point. This situation makes possible adequate control of ring-groove-pad temperatures through the use of thin sections of a low conductivity material such as steel, or any modifications such as "heat dam" construction, without adverse effect on crown temperature. It is then possible to develop light-weight designs subject only to limitations such as strength, rigidity, or fabrication. Provision for additional oil-cooling requirements may be necessary in some cases, but freedom from performance restriction would prove a sufficient compensation.

An example of such performance restriction was found in a recent German aircraft engine. The piston of this engine limited operation to a mean effective pressure 30 pounds per square inch below the knock-limited mean effective pressure of the fuel used. Attempted operation near the knock limit resulted in excessive piston-crown temperature of the order of 650° F, as well as severe piston-ring distress. The design of this piston was similar to the one shown in figure 1 (a). It can be seen from figure 12 that with a low value of k_o (for example, 1 Btu/(hr) (sq in.) (°F)) and with a highly conductive path from the center crown to the ring-groove-pad section, the indicated center-crown (hot-spot) temperature for the assumed conditions of the analysis could readily attain a temperature of 650° F, with a corresponding ring-

groove-pad temperature on the order of 500° F, which is considered excessive.

The evolution of piston designs that alleviated ring distress resulting from excessive temperature took place in two distinct ways. In one case, as piston-temperature limits were reached, various auxiliary cooling devices were introduced, the principal ones being use of oil jets against the undercrown surface or positive circulation through the piston body. Where jets were used, the design of the piston was altered to provide minimum ring-groove-pad temperatures by using thin sections, as indicated in figure 12; in a two-cycle Diesel engine the material was changed to steel. Representative investigations of this nature are reported in references 5 and 6. The other course of development was based on the discovery that high undercrown coefficients were normal in some engines, and as reported in reference 7, the piston design was altered in a similar manner to take fullest advantage of the available cooling.

With regard to the heat balance of the piston, careful consideration shows that it is not necessarily a good criterion of piston-temperature distribution. It is possible in the case of a thin cast-iron piston operating with a low undercrown coefficient and with low radial conductivity that the heat balance will show a preponderance of flow in the direction of the crankcase by virtue of the excessive crown temperature. Similarly, an aluminum piston with heavy sections and high radial conductivity might show a preponderance of flow in the direction of the cylinder wall and an excessive ring-groove-pad temperature, even though the available undercrown cooling is adequate to permit substantial reduction in the ring-groove-pad temperature by design alteration without increase in crown temperature. The heat balance after such design changes would show a preponderance of flow in the direction of the crankcase atmosphere.

The heat balance for the piston-cooling load, given in table II, is computed from the analytically determined temperature distribution for the operating conditions previously specified and in the data presented in table I and in figure 9.

TABLE II—HEAT BALANCE FOR PISTON-COOLING LOAD

Location	Dissipation (percent)
Heat dissipation from undercrown surface.....	71
Heat dissipation from undercrown surface behind ring-groove pad..	11
Heat dissipation from upper- and lower-skirt sections.....	10
Heat dissipation from rings and lands.....	8

The total heat flow through the piston crown amounts to roughly 17,300 Btu per hour, or about 2 percent of the energy represented by the heating value of the fuel consumed. The direct effect of the cooling on thermal efficiency of the engine is therefore small. A large part of this heat loss represents heat transferred to the piston during the exhaust process; therefore the direct loss of what would otherwise be available energy is probably considerably less than 1 percent of the total heat input.

CONCLUSIONS

From an analysis of piston-temperature variation with piston geometry for a specific set of boundary conditions, it is concluded that:

1. Piston temperature can be effectively controlled by increasing the undercrown-surface heat-transfer coefficient with resulting possibilities for light-weight designs consistent with requirements of strength, rigidity, or fabrication, and with freedom from restrictions of large high-conductivity sections and materials of high thermal conductivity.

2. When available undercrown cooling is limited, reduction of either crown temperature or ring-groove-pad temperature through design alteration is restricted by the adverse effect on the other.

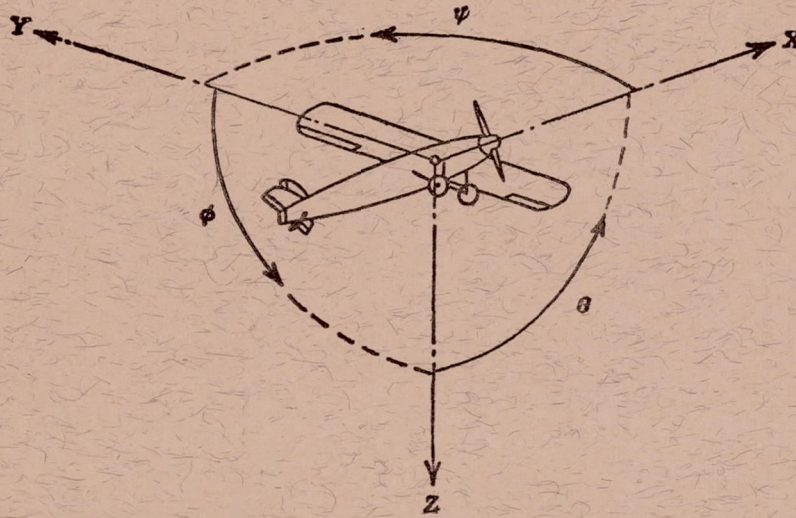
3. The methods employed permit satisfactory determination of piston-temperature distribution by analytical methods in specific cases where boundary conditions are known.

4. The heat balance may show preponderance of flow in the direction of the cylinder wall or crankcase atmosphere depending on the piston design and cooling arrangement, and bears no direct relation to the temperature distribution that may be encountered.

FLIGHT PROPULSION RESEARCH LABORATORY,
NATIONAL ADVISORY COMMITTEE FOR AERONAUTICS,
CLEVELAND, OHIO, *January 15, 1948.*

REFERENCES

1. Gibson, A. H.: Piston Temperatures and Heat Flow in High-Speed Petrol Engines. *Engineering*, vol. CXXI, nos. 3135-3136, Jan. 29 and Feb. 5, 1926, pp. 150-152, pp. 183-185.
2. Baker, H. Wright: A Study of Piston Temperatures and Their Relation to Piston Design. *Proc. Inst. Auto. Eng. (London)*, vol. 27, Nov. 1932, pp. 109-138.
3. Huebotter, H. A., and Young, G. A.: Flow of Heat in Pistons. *Bull. No. 25, Purdue Univ. Eng. Exp. Station Bull.*, vol. IX, no. 12, Dec. 1925.
4. Janeway, R. N.: Quantitative Analysis of Heat Transfer in Engines. *SAE Jour. (Trans.)*, vol. 43, no. 3, Sept. 1938, pp. 371-380.
5. Flynn, Gregory, Jr., and Underwood, Arthur F.: Adequate Piston Cooling—Oil Cooling as a Means of Piston Temperature Control. *SAE Jour. (Trans.)*, vol. 53, no. 2, Feb. 1945, pp. 120-128.
6. Keyser, P. V., Jr., and Miller, E. F.: Piston and Piston Ring Temperatures. *Jour. Inst. Petroleum*, vol. 25, no. 194, Dec. 1939, pp. 779-790.
7. Gosslau, F.: Development of High Duty Pistons Based on Modern Researches on Heat Flow. *British R. T. P. Trans. No. 1669, Ministry Aircraft Prod. (From Auto. tech. Zeitschr., Jahrg. 44, Nr. 24, Dez. 20, 1941.)*
8. Willis, E. J., and Anderson, R. G.: Operating Temperatures and Stresses in Aluminum Aircraft-Engine Parts. *SAE Trans.*, vol. 52, no. 1, Jan. 1944, pp. 28-36.
9. Paschkis, Victor, and Baker, H. D.: A Method for Determining Unsteady-State Heat Transfer by Means of an Electrical Analogy. *Trans. ASME*, vol. 64, no. 2, Feb. 1942, pp. 105-112.
10. Pinkel, Benjamin: Heat-Transfer Processes in Air-Cooled Engine Cylinders. *NACA Rep. No. 612, 1938.*
11. Manganiello, Eugene J., and Bogart, Donald: Piston Heat-Transfer Coefficients across an Oil Film in a Smooth-Walled Piston Reciprocating-Sleeve Apparatus. *NACA ARR No. E5K08, 1945.*



Positive directions of axes and angles (forces and moments) are shown by arrows

Axis		Force (parallel to axis) symbol	Moment about axis			Angle		Velocities	
Designation	Symbol		Designation	Symbol	Positive direction	Designation	Symbol	Linear (component along axis)	Angular
Longitudinal.....	X	X	Rolling.....	L	Y → Z	Roll.....	φ	u	p
Lateral.....	Y	Y	Pitching.....	M	Z → X	Pitch.....	θ	v	q
Normal.....	Z	Z	Yawing.....	N	X → Y	Yaw.....	ψ	w	r

Absolute coefficients of moment

$$C_l = \frac{L}{qbS} \quad C_m = \frac{M}{qcS} \quad C_n = \frac{N}{qbS}$$

(rolling) (pitching) (yawing)

Angle of set of control surface (relative to neutral position), δ. (Indicate surface by proper subscript.)

4. PROPELLER SYMBOLS

D	Diameter	P	Power, absolute coefficient $C_P = \frac{P}{\rho n^3 D^5}$
p	Geometric pitch	C_s	Speed-power coefficient = $\sqrt[5]{\frac{\rho V^5}{P n^2}}$
p/D	Pitch ratio	η	Efficiency
V'	Inflow velocity	n	Revolutions per second, rps
V _s	Slipstream velocity	φ	Effective helix angle = $\tan^{-1} \left(\frac{V}{2\pi r n} \right)$
T	Thrust, absolute coefficient $C_T = \frac{T}{\rho n^2 D^4}$		
Q	Torque, absolute coefficient $C_Q = \frac{Q}{\rho n^2 D^5}$		

5. NUMERICAL RELATIONS

1 hp = 76.04 kg-m/s = 550 ft-lb/sec	1 lb = 0.4536 kg
1 metric horsepower = 0.9863 hp	1 kg = 2.2046 lb
1 mph = 0.4470 mps	1 mi = 1,609.35 m = 5,280 ft
1 mps = 2.2369 mph	1 m = 3.2808 ft

